Inorganic Chemistry

Article

pubs.acs.org/IC

New Synthetic Routes to Iron−Sulfur Clusters: Deciphering the Repair Chemistry of [2Fe−2S] Clusters from Mononitrosyl Iron Complexes

Jessica Fitzpatrick and Eunsuk Kim*

Department of Chemistry, Brown University, 324 Brook Street, Providence, Rhode Island 02912, United States

Supporting Information

ABSTRACT: The nitrosylation of inorganic protein cofactors, specifically that of [Fe−S] clusters to form iron nitrosyls, plays a number of important roles in biological systems. In some of these cases, it is expected that a repair process reverts the nitrosylated iron species to intact [Fe−S] clusters. The repair of nitrosylated [2Fe−2S] cluster, primarily in the form of protein-bound dinitrosyl iron complexes (DNICs), has been observed *in vitro* and *in vivo*, but the mechanism of this process remains uncertain. The present work expands upon a previous observation (Fitzpatrick et al. *J. Am. Chem. Soc.* **2014**, *136*, 7229) of the ability of mononitrosyl iron complexes (MNICs) to be converted into [2Fe−2S] clusters by the addition of nothing other than a cysteine analogue. Herein, each of the critical elementary steps in the cluster repair has been dissected to elucidate the roles of the cysteine analogue. Systematic variations of a cysteine analogue employed in the repair reaction suggest that (i) the bidentate coordination of a cysteine analogue to MNIC promotes NO release from iron, and (ii) deprotonation of the α carbon of the ferric-bound cysteine analogue leads to the C−S cleavage en route to the formation of [2Fe−2S] cluster. The [2Fe−2S] cluster bearing a cysteine analogue has also been synthesized from thiolate-bridged iron dimers of the form $[Fe_2(\mu\text{-}SR)_2(SR)_4]^{0/2-}$, which implies that such species may be present as intermediates in the cluster repair. In addition to MNICs, mononuclear tetrathiolate ferric or ferrous species have been established as another form of iron from which [2Fe−2S] clusters can be generated without need for any other reagent but a cysteine analogue. The results of these experiments bring to light new chemistry of classic coordination complexes and provides further insight into the repair of NO-modified [2Fe−2S] clusters.

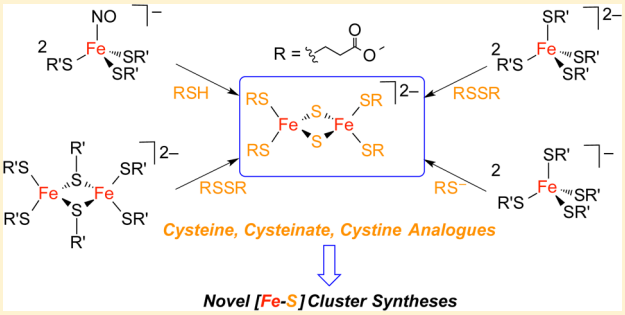

1. INTRODUCTION

Nitric oxide (NO) plays important roles in many biological processes[1] including, but not limited to, vasoregulation,[2] immunity,[3] and neurotransmission.[4] Many of these functions arise from the interaction of NO with metal centers in biological systems, such as the cofactors of metalloproteins. The study of NO as a ligand in coordination chemistry has a long history, albeit one complicated by the noninnocence that it often exhibits.[5,6] A class of complexes that exemplifies the effects of this noninnocence on structure and bonding comprises the dinitrosyl iron complexes (DNICs). As a result of their electronic structures, these molecules display characteristic EPR signals.[7−9] This spectroscopic handle led to a series of discoveries that revealed the biological relevance of DNICs of the form $[Fe(NO)_2X_2]^{-/0}$, where the X ligand can be a free thiolate, the thiolates of cysteine residues of a protein, or the imidazoles of histidine residues of a protein.[10−16] One source of protein-bound DNICs is the interaction of NO with [Fe−S] cluster cofactors of certain metalloproteins.[8,17,18] The conversion of [Fe−S] cluster to DNIC can bring about significant changes in protein function. For example, the SoxR protein found in *Escherichia coli* bears a [2Fe−2S] cluster that decomposes to form protein-bound DNIC upon exposure to NO.[19] Formation of the DNIC activates this protein to function as a transcription activator for the *soxS* gene, another transcription factor whose product promotes the expression of a large group of defensive proteins that increase the ability of the microorganism to survive oxidative stress.[19] Other systems in which the conversion of [Fe−S] clusters to DNICs has been proposed to play a functional role include the bacterial NO sensor-regulator NsrR,[20−22] and the WhiB-like (Wbl) family of regulatory proteins found in actinomycetes.[23,24] Conversely, the interaction of NO with aconitases can be destructive rather than functional because nitrosylation of the active-site [4Fe−4S] cluster abrogates enzymatic activity and interrupts a vital metabolic process.[25,26] This metabolic disruption may be an important mechanism by which the NO released by macrophages at sites of infection kills pathogenic microorganisms.

For cells to employ NO as an effective signaling agent or to better survive immunological attacks, it is logical to propose that a DNIC-to-[Fe−S] cluster transformation may exist (Scheme 1). Evidence for such repair was observed in whole-cell EPR spectroscopic experiments performed on *E. coli*

Received: April 28, 2015
Published: June 18, 2015

DOI: 10.1021/acs.inorgchem.5b00961
Inorg. Chem. 2015, 54, 10559−10567

Scheme 1. [Fe−S] Clusters and Protein-Bound DNICs Can Interconvert

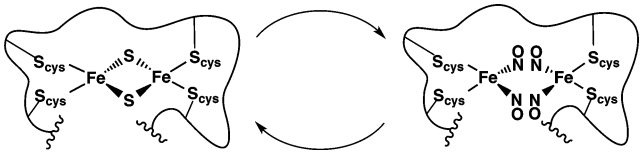

overexpressing SoxR.[19] Exposure of the cells to NO gas resulted in disappearance of the EPR signal from the mixed-valent [2Fe−2S] cluster of SoxR and its replacement by a characteristic DNIC signal. Continued incubation of the cells in the absence of NO resulted in conversion of the DNIC EPR signal back to that of the intact [Fe−S] cluster. Related *in vitro* experiments with [2Fe−2S] ferredoxin revealed that isolated protein-bound DNIC could be converted to protein with intact [2Fe−2S] cluster upon aerobic incubation with cysteine and cysteine desulfurase.[27,28] Importantly, no additional iron was added to the system, indicating that the iron present in the DNIC was recycled to form the [Fe−S] cluster. The detailed mechanism by which these transformations occur, however, remains unknown.

One approach used to gain insight into these biochemical transformations is to investigate the reactivity of small-molecule models of these bioinorganic species. Investigation of the interaction of NO with [Fe−S] clusters has benefitted greatly from the extensive work carried out by many researchers, perhaps most notably those of the Holm group, to investigate the inorganic syntheses of small-molecule [Fe−S] clusters.[29,30] The reactivity of these complexes has provided significant insight into the biosynthesis of their protein-bound counterparts and the reactions that such metalloproteins undergo. Small-molecule [2Fe−2S] clusters are typically prepared by reaction of ferric or ferrous tetrathiolate complexes with elemental sulfur.[30] An alternative strategy involves the reaction of ferric chloride, thiolate, hydrosulfide, and methoxide.[30] Reaction of such synthetic [2Fe−2S] clusters with NO typically affords DNICs.[9,31] The opposing reaction, in which a DNIC is converted into a [2Fe−2S] cluster, has also been investigated.[32,33] For example, the DNIC $[Fe(NO)_2(S_5)]^-$ could be irradiated with UV light to photolytically release NO, which was trapped by an exogenous Fe-based NO-acceptor.[32] If the photolysis is carried out in the presence of elemental sulfur, then the corresponding [2Fe−2S] cluster re-forms.[32] In light of the known NO reactivity of tetrathiolatoiron(II) complexes in which 1 equiv produces a mononitrosyl iron complex (MNIC), whereas 2 equiv produces a DNIC,[34] we were intrigued by the possibility that MNICs could be intermediates in the conversion of DNICs to [2Fe−2S] clusters.

We recently reported that MNICs with alkylthiolate ligands are converted into [2Fe−2S] clusters following addition of nothing other than the cysteine analogue methyl 3-mercaptopropionate (MMP) (Scheme 2).[35] Subsequent experiments revealed that the sulfur atoms of the bridging sulfides of the [2Fe−2S] cluster originate from MMP. Careful analysis of the other reaction products revealed that a DNIC and the thioether $S(CH_2CH_2C(O)OMe)_2$ were also generated at the end of the reaction, Scheme 3.

In our previous report, we proposed that a thiolate-bridged Fe(II) dimer of the form $[Fe(\mu\text{-}SR)(SR)_2]_2^{2-}$ (**5**) might be an intermediate in the transformation (Scheme 3). Our initial proposal of **5** as an intermediate was largely based on product

Scheme 2. Conversion of MNIC to [2Fe−2S] Cluster Upon Addition of the Cysteine Analogue, MMP

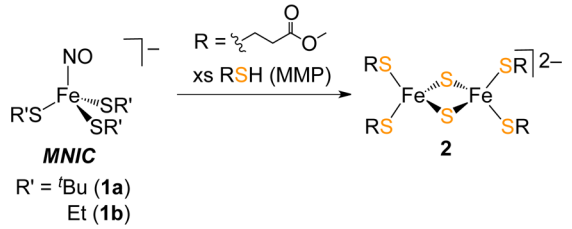

Scheme 3. Previously Proposed Mechanism of the MNIC-to-[2Fe−2S] Cluster Transformation

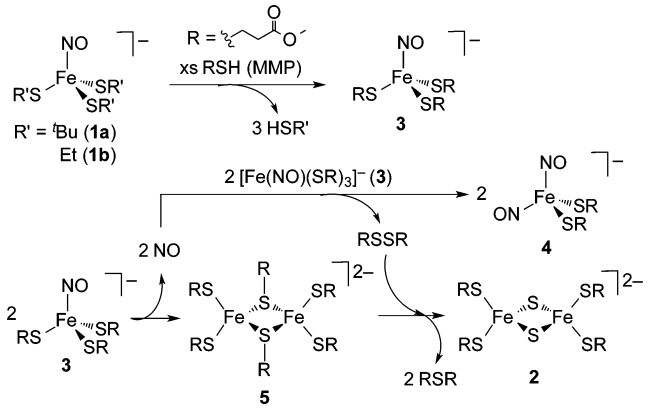

analysis because no intermediates build up in the course of the reaction. In this current work, we provide a detailed characterization of each of the elementary steps by which thiolate-bridged ferrous dimers can form [2Fe−2S] clusters upon addition of a cysteine analogue or both a cysteine analogue and an exogenous oxidant. We have also further explored the scope of this reactivity to probe the mechanism by which the MNIC-to-[2Fe−2S] cluster transformation occurs and to uncover which molecular features of the cysteine analogues permit this reactivity. The results of these experiments are consistent with those of our previously proposed model of the conversion of MNIC to the [2Fe−2S] cluster and allowed us to uncover a reactivity of these classic complexes that has remained unappreciated until now. In this way, these results not only add to the repertoire of fascinating chemistry available to iron thiolate compounds, but also corroborate our hypothesis that such species may play key roles in the bioinorganic chemistry of iron nitrosyl complexes.

2. RESULTS AND DISCUSSION

2.1. Coordination of a Cysteine Analogue to Fe Assists NO Release from Mononitrosyl Iron Complexes (MNICs). The MNIC-to-[2Fe−2S] cluster transformation involves release of NO from the iron center. Previous computational studies[35] on an MMP-ligated MNIC suggested that bidentate coordination of iron by MMP positions the sulfur atom of MMP *trans* to NO, which promotes the release of NO• (Scheme 4). To further validate this idea, we carried out reactions of $[Fe(NO)(S^tBu)_3]^-$ (**1a**) with various types of thiols including several cysteine analogues (Table 1).

Addition of simple thiols or thiolates such as alkyl or aryl thiol derivatives to **1a** or **1b** did not lead to the formation of [2Fe−2S] clusters. In fact, the $\{Fe(NO)\}^7$ unit in the MNIC is quite robust and persists in the presence of a wide range of

DOI: 10.1021/acs.inorgchem.5b00961
Inorg. Chem. 2015, 54, 10559−10567

Scheme 4. Participation of 5-Coordinate Isomer in the Formation of [2Fe−2S] Cluster

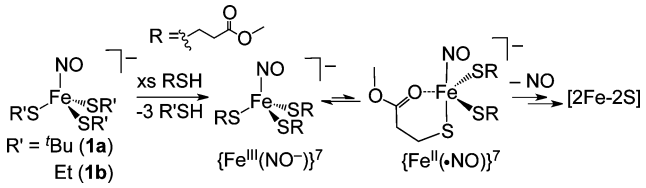

Table 1. Ability of Different Thiols To Mediate Formation of [2Fe−2S] Cluster

Thiol	Cluster Formation (% Yield)[a]
	no
	no
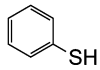	no
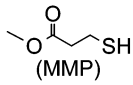 (MMP)	yes (45%)
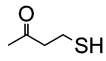	yes (40%)
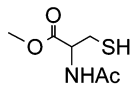	yes (37%)

[a]The maximum theoretical yield of cluster in these reactions is 50% given the reaction stoichiometry shown in Scheme 3.

thiols or thiolates. Many of these thiols and thiolates can, however, substitute for the thiolate ligands of MNIC. For example, addition of a thiol that is more acidic than *tert*-butyl thiol to the starting **1a** leads to thiolate ligand exchange, analogous to the well-known ligand exchange chemistry of [Fe−S] clusters.[30] Literature precedent suggests that removal of NO from an iron nitrosyl by a thiolate would be feasible via nucleophilic attack on the iron-bound nitrosyl when an NO ligand is present with NO^+ character.[36,37] Therefore, the lack of success in removing NO from **1a** by addition of simple thiol/thiolate is perhaps unsurprising because **1a** has already been well-established as an $\{Fe(III)(NO^-)\}^7$ complex[34] rather than an $\{Fe(I)(NO^+)\}^7$ species.

The stability of the $\{Fe(NO)\}^7$ unit of **1a** disappears when cysteine analogues are added. For instance, when a THF or acetonitrile solution of $(PPN)[Fe(NO)(S^tBu)_3]$ (PPN-**1a**), where PPN = bis(triphenylphosphine)iminium, is allowed to react with an excess of a cysteine analogue, such as MMP, $HSCH_2CH_2C(O)Me$, or *N*-acetylcysteine methyl ester (Table 1), the red-brown solution turns brown and IR spectra of the reaction mixture reveal that no MNIC remains. If the reaction with MMP is carried out in THF, the final [2Fe−2S] cluster, $(PPN)_2[Fe_2S_2(SCH_2CH_2C(O)OMe)_4]$ ($(PPN)_2$-**2**), can be readily isolated from the reaction mixture.[38] An alternative method of isolating $(PPN)_2$-**2** involving elaborate serial recrystallizations has been reported earlier.[35] In contrast to the reaction with MMP, all of the products of the reactions involving other cysteine analogues, $HSCH_2CH_2C(O)Me$ and *N*-acetylcysteine methyl ester, with **1a** or **1b** are readily soluble in THF, precluding facile isolation as was possible with MMP. Stripping these reaction mixtures of volatile components, washing with a 1:1 mixture of THF and diethyl ether, and dissolving the residue in acetonitrile afforded solutions with electronic absorption and FTIR spectra consistent with the formation of the corresponding [2Fe−2S] clusters (Supporting Information Figures S1−S4). The THF−diethyl ether wash removes the DNIC byproduct that is formed, and the excess thiol is removed under vacuum.

The data collected to date suggest that two features of the thiol added to the MNIC are required for release of NO en route to [2Fe−2S] cluster formation. The first is that the thiol must be able to substitute for the thiolate ligands initially bound to the iron center. This property can be related to the pK_a of the thiol. Indeed, MMP (pK_{aSH} = 9.33 in 50% water−50% DMSO)[39] is unable to produce the cluster from PhS-bound MNIC, $[Fe(NO)(SPh)_3]^-$ (pK_{aSH} = 6.6 in water).[40,41] Once substitution at the metal center has occurred, pK_a appears to no longer be a decisive factor in cluster formation. For instance, EtSH, MMP, and $HSCH_2CH_2C(O)Me$ are expected to have very similar pK_a values and yet only the latter two, cysteine analogues, can form cluster. The conspicuous difference between the thiols/thiolates that can effect formation of [2Fe−2S] cluster and those that cannot is the presence or absence, respectively, of the carbonyl moiety. These results are consistent with our previous proposal that the 5-coordinate isomer (Scheme 4) is the key species to remove NO from iron to eventually generate the [2Fe−2S] cluster. The NO releasing chemistry observed here is in line with the known ability of thiolate ligands of heme and nonheme iron complexes to labilize *trans* ligand including $NO^{\bullet}$.[42,43] The NO released from MNIC can then interact with another equivalent of MNIC generating a DNIC and a thiolate-bridged ferrous dimer (Scheme 3).

2.2. [2Fe−2S] Clusters Can Be Generated from a Bis(μ-thiolato) Differous Precursor. Once NO is released from $\{Fe(NO)\}^7$ MNIC, the resulting ferrous moiety is presumed to form a thiolate-bridged species, **5**, Scheme 3. To probe the possibility that such a thiolate-bridged ferrous dimer, **5**, can function as a viable reaction intermediate, we have independently synthesized a known[44] ethyl analogue $(PPN)_2[Fe_2(\mu\text{-}SEt)_2(SEt)_4]$ ($(PPN)_2$-**5a**) and investigated the reaction of **5a** with $(SCH_2CH_2C(O)OMe)_2$ (Scheme 5).

Scheme 5. Thiolate-Bridged Fe(II) Dimer as a Precursor to [2Fe−2S] Cluster

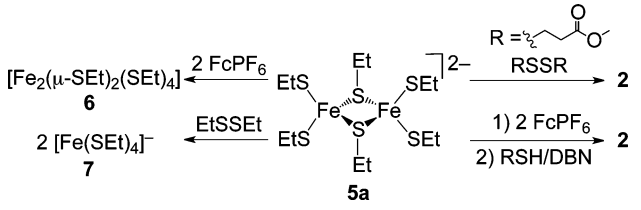

Addition of this disulfide to an acetonitrile solution of **5a** induced a rapid change in the color of the solution. The near colorless solution of **5a** immediately acquired a deep red-brown color (λ_{max} = 470 nm) and then more slowly changed to a final true brown color (Figure 1). The spectrum of the final solution, with absorption maxima at 330, 425, and 450 nm, corresponds to that of the [2Fe−2S] cluster that we have previously reported, $[Fe_2(\mu\text{-}S)_2(SCH_2CH_2C(O)OMe)_4]^{2-}$ (**2**).[35]

DOI: 10.1021/acs.inorgchem.5b00961
Inorg. Chem. 2015, 54, 10559−10567

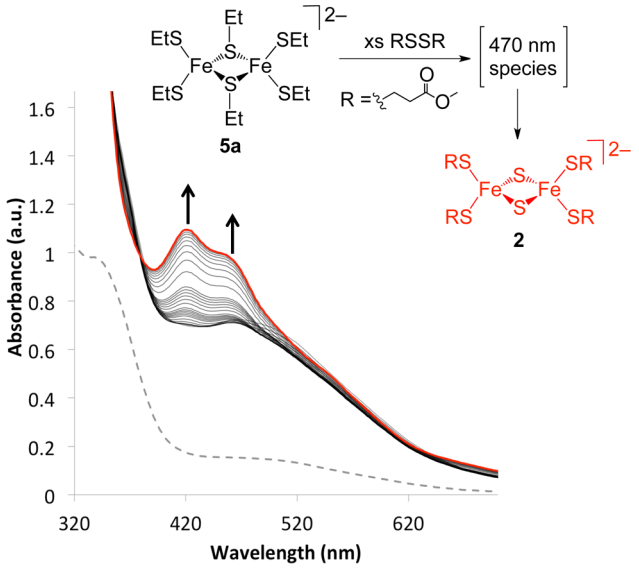

Figure 1. UV−vis spectral changes associated with the reaction of $[Fe_2(\mu\text{-SEt})_2(SEt)_4]^{2-}$ (**5a**) (dashed trace) and an excess of $(SCH_2CH_2C(O)OMe)_2$ to yield the rapid formation of a red-brown species with λ_{max} = 470 nm (black trace) followed by a slow formation of $[Fe_2(\mu\text{-S})_2(SCH_2CH_2C(O)OMe)_4]^{2-}$ (**2**) (red trace) in acetonitrile at room temperature over the course of 6 h.

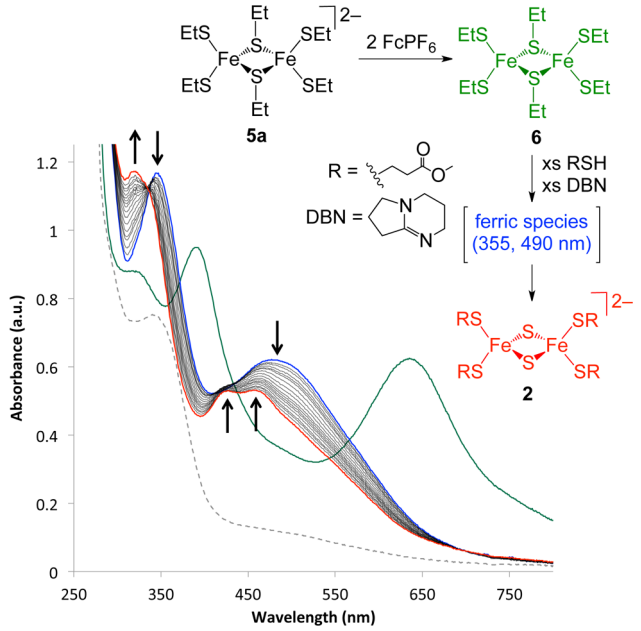

Figure 2. UV−vis spectral changes associated with the reaction of $[Fe_2(\mu\text{-SEt})_2(SEt)_4]^{2-}$ (**5a**) (dashed trace) and 2 equiv of $FcPF_6$ to form a putative $[Fe_2(\mu\text{-SEt})_2(SEt)_4]$ (**6**) (green trace), followed by addition of excess MMP and DBN to yield another ferric intermediate species (blue trace) which converts to $[Fe_2(\mu\text{-S})_2(SCH_2CH_2C(O)OMe)_4]^{2-}$ (**2**) (red trace) in acetonitrile at room temperature. Total reaction time was 20 min.

In addition to small-scale experiments designed to spectroscopically monitor the progress of this reaction, the conversion of $(PPN)_2[Fe_2(\mu\text{-SEt})_2(SEt)_4]$ ($(PPN)_2$-**5a**) to $(PPN)_2[Fe_2(\mu\text{-S})_2(SCH_2CH_2C(O)OMe)_4]$ ($(PPN)_2$-**2**) was also carried out on a preparative scale. Similarly to the method employed to isolate **2** from the reaction of MMP and $[Fe(NO)(^tBuS)_3]^-$ (**1**) as described in section 2.1, pure product **2** from the reaction of **5a** with $(SCH_2CH_2C(O)OMe)_2$ was obtained by exploiting differential solubility of the starting materials and product. If 20 equiv of $(SCH_2CH_2C(O)OMe)_2$ are added to a THF solution of **5a**, then the [2Fe−2S] cluster **2** simply precipitates from solution over the course of 4 h. Starting from a THF solution of $(PPN)_2[Fe_2(\mu\text{-SEt})_2(SEt)_4]$ (**5a**), analytically pure [2Fe−2S] cluster can be obtained in 76% yield simply by filtering the reaction mixture. The spectroscopic features of this material are consistent with those obtained in the monitoring experiments or preparative reactions in acetonitrile.

In contrast to the evident reaction that occurs upon addition of a disulfide, $(SCH_2CH_2C(O)OMe)_2$, addition of a related thiol, MMP, to a solution of $[Fe_2(\mu\text{-SEt})_2(SEt)_4]^{2-}$ (**5a**) results in no cluster formation. In order to probe whether the formation of the [2Fe−2S] cluster from **5a** depends on the ability of $(SCH_2CH_2C(O)OMe)_2$ to act as an oxidant, we combined **5a** with 2 equiv of ferrocenium (Fc^+) followed by an excess of $^-SCH_2CH_2C(O)OMe$, generated *in situ* by combining MMP and the base 1,5-diazabicyclo[4.3.0]non-5-ene (DBN), Scheme 5. Optical absorption spectroscopic measurements were used to follow the progress of this stepwise reaction (Figure 2). Addition of the 2 equiv of ferrocenium (Fc^+) to **5a** results in the formation of a green species with absorption maxima at 320, 390, and 635 nm. We propose that this green complex is the corresponding thiolate-bridged ferric dimer, $[Fe_2(\mu\text{-SEt})_2(SEt)_4]$ (**6**), Scheme 5. Addition of MMP and DBN to this solution results in an immediate color change with the appearance of new absorption maxima at 355 and 490 nm, which is reminiscent of tetrathiolatoiron(III) species, $[Fe(SCH_2CH_2C(O)OMe)_4]^-$. This species subsequently transforms to $[Fe_2(\mu\text{-S})_2(SCH_2CH_2C(O)OMe)_4]^{2-}$ (**2**) over the next 20 min (Figure 2) and can be isolated in a 45% yield. We note briefly that dioxygen instead of Fc^+ can also be effectively used as the oxidant in these reactions, affording the product with a 56% isolated yield. The justification for using the thiolate form of MMP will be provided below, but here we highlight that if the thiol is not deprotonated, and then the reaction stops at the formation of the green intermediate, **6**, and does not proceed to give cluster. Regrettably, we have been unable to isolate the proposed diferric intermediate, $[Fe_2(\mu\text{-SEt})_2(SEt)_4]$ (**6**), because the complex appears to be unstable. However, the Holm group has reported a series of analogous green compounds with the empirical formula $[Fe(SR)_3]_n$, where R is Me, Et, CH_2Ph, or $CH_2C_6H_{11}$ although the exact structures have not been elucidated.[45] The formation of such $Fe(SR)_3$ species was also reported by the Henkel group.[46] We assign absorption features that give the intermediate solution a green color to a diferric species as opposed to a mixed-valent complex because addition of only 1 equiv of ferrocenium to the diferrous complex produces absorption features with half the intensity and addition of the second equivalent of ferrocenium produces the full intensity peaks (Supporting Information Figure S5). We note that, at each stage of this two-step titration, the absorbance from the added ferrocenium is completely extinguished, indicating full consumption of the oxidant.

Although the putative diferric thiolate-bridged intermediate, $[Fe_2(\mu\text{-SEt})_2(SEt)_4]$ (**6**), observed during the reaction of Fc^+ and the ferrous dimer could not be isolated, the corresponding monomeric tetrathiolatoiron(III) complexes are readily prepared. If $(PPN)[Fe(SEt)_4]$ (PPN-**7**) is combined with MMP, no reaction other than ligand substitution occurs. If added to

DOI: 10.1021/acs.inorgchem.5b00961
Inorg. Chem. 2015, 54, 10559−10567

MMP and DBN, however, clean conversion to the [2Fe−2S] cluster takes place (Figure 3), and the product can be isolated in an 85% yield. The significance of this reaction condition is described in the following section.

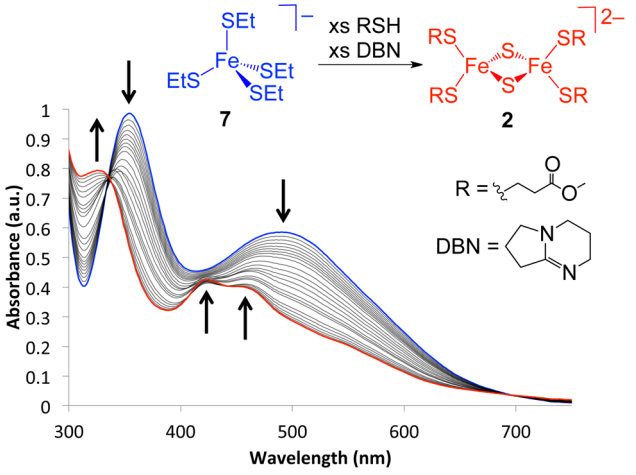

Figure 3. UV−vis spectral changes associated with the reaction of $[Fe(SEt)_4]^-$ (**7**) (blue trace), 50 equiv of MMP, and 50 equiv of DBN in acetonitrile at room temperature to form the corresponding [2Fe−2S] cluster, $[Fe_2(\mu\text{-}S)_2(SCH_2CH_2C(O)OMe)_4]^{2-}$ (**2**) (red trace). The total reaction time was 35 min.

2.3. Deprotonation of Cysteine Analogue Leads to the C−S Cleavage To Form [2Fe−2S] Cluster. As described in section 2.1, the transformation of MNIC to [2Fe−2S] cluster by cysteine analogues depends on the ability of these molecules to form 5-coordinate isomers of the MNIC via coordination of the carbonyl oxygen atom. Two other results from the product analyses indicate that some other characteristic features of the cysteine analogue are essential for the transformation in question. The first is the observation that the bridging sulfides in the [2Fe−2S] cluster originated from MMP.[35] The second is the quantitative formation of the thioether analogue of MMP, $S(CH_2CH_2C(O)OMe)_2$ during the reaction (Scheme 3).[35] These observations imply that the C−S bond of MMP is cleaved in the reaction of MNIC with MMP. The analogous reaction of $[Fe(NO)(S^tBu)_3]^-$ (**1a**) with EtSH produces no cluster and the reaction of $[Fe_2(\mu\text{-}SEt)_2(SEt)_4]^{2-}$ (**5a**) with EtSSEt produces only $[Fe(SEt)_4]^-$ (**7**) (Scheme 5, Supporting Information Figure S6). Given the similarities in the pK_{aSH} values and redox potentials of EtSH and MMP, some other feature of MMP must be giving rise to the observed reactivity. We suggest that this feature is the acidity of the proton on the α-carbon.

We propose that, in the transformation of $[Fe(SEt)_4]^-$ (**7**) to $[Fe_2(\mu\text{-}S)_2(SCH_2CH_2C(O)OMe)_4]^{2-}$ (**2**) as described in the previous section (Figure 3), a base (DBN or the thiolate form of MMP) deprotonates the α-carbon of the Fe-coordinated MMP (Scheme 6). Consequent heterolytic cleavage of the C−S bond provides an Fe-coordinated sulfide (S^{2-}) which is required in the final [2Fe−2S] cluster product, as well as an equivalent of methyl acrylate (Scheme 6). Reaction of MMP with methyl acrylate results in the quantitative formation of the thioether form of MMP, $S(CH_2CH_2C(O)OMe)_2$. We have independently confirmed that addition of MMP to a solution of methyl acrylate produces $S(CH_2CH_2C(O)OMe)_2$.

Scheme 6. Deprotonation of Fe-Bound Thiolate Drives C−S Bond Cleavage and Formation of the [2Fe−2S] Cluster

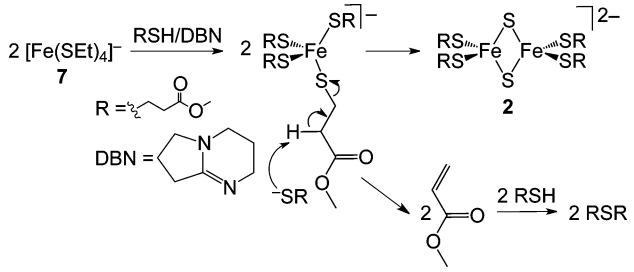

To test the hypothesis that deprotonation of the α-carbon of MMP is crucial for the formation of the [2Fe−2S] cluster from both ferrous and ferric precursors, $[Fe_2(\mu\text{-}SEt)_2(SEt)_4]^{2-}$ (**5a**) and $[Fe(SEt)_4]^-$ (**7**), respectively, analogues of $(SCH_2CH_2C(O)OMe)_2$ and MMP were used that differ from these compounds in key respects with regard to proton position and acidity. If the orientation of the ester linkage is reversed, as in the case of $HSCH_2\mathbf{CH_2}OC(O)Me$, the CH_2 unit highlighted in bold has lowered acidity[47,48] and cannot be readily deprotonated. Accordingly, addition of the disulfide form of $HSCH_2CH_2OC(O)Me$ to a solution of **5a** results in no cluster formation. If, alternatively, the carbon chain between the sulfur atom and the carbonyl functional group is lengthened by one methylene unit, as in $(SCH_2CH_2CH_2C(O)OMe)_2$, again no cluster was observed upon addition to **5a**. The lack of cluster formation in this latter case arises from the fact that the acidic proton is no longer properly positioned for carbon−sulfur bond breaking. We have found, however, that analogues of MMP in which the protons of the α-carbon are appropriately acidic[47] and properly positioned do lead to cluster formation. For example, $HSCH_2CH_2C(O)Me$ is a ketone analogue of MMP that forms the corresponding [2Fe−2S] cluster when added to **7** in the presence of DBN (Supporting Information Figure S7). Moreover, the greater acidity of the α-carbon of $HSCH_2CH_2C(O)Me$, as compared to MMP, is reflected in the greater rate at which the starting material is consumed in the former case (Supporting Information Figure S8). Similarly, *N*-acetylcysteine methyl ester forms a [2Fe−2S] cluster upon reaction with **7** and DBN, but appears to also participate in a side reaction, as evidenced by the lack of clear isosbestic points (Supporting Information Figure S9), precluding a comparison of the rate of this reaction with those of the other cysteine analogues. As described in section 2.1, these two cysteine analogues are also able to generate [2Fe−2S] cluster upon reaction with MNIC. Formation of [2Fe−2S] cluster from tetrathiolatoiron(III) and the cysteine analogues could be followed by electronic absorption monitoring experiments. The spectra of the final solutions match those of the products obtained from the reactions with MNIC (*vide supra*) and from independently prepared samples of the clusters synthesized by ligand substitution of the $(PPN)_2[Fe_2(\mu\text{-}S)_2(S^tBu)_4]$ with the corresponding thiol (Supporting Information Figures S7−S8). These clusters have proven to be highly unstable. Although they persist in solution long enough to permit spectral characterization, and in the solid state at −35 °C for ca. 12 h, we have yet been unable to further characterize these clusters.

With the insight gained from the reactions with monomeric tetrathiolatoiron(III) complexes, we can revisit the working model for the MNIC-to-[2Fe−2S] cluster transformation

DOI: 10.1021/acs.inorgchem.5b00961
Inorg. Chem. 2015, 54, 10559−10567

depicted in Scheme 3 and propose a mechanism for the final step of the reaction (Scheme 7). Reaction of $[Fe_2(\mu\text{-}SR)_2(SR)_4]^{2-}$ (**5**) with $(SCH_2CH_2C(O)OMe)_2$ oxidizes **5** to the diferric state, generating free thiolate. The released thiolate deprotonates the α-carbon of the bridging thiolate of **6** triggering C–S bond cleavage and formation of the [2Fe–2S] cluster.

Scheme 7. Role of Deprotonation in the [2Fe–2S] Cluster Repair

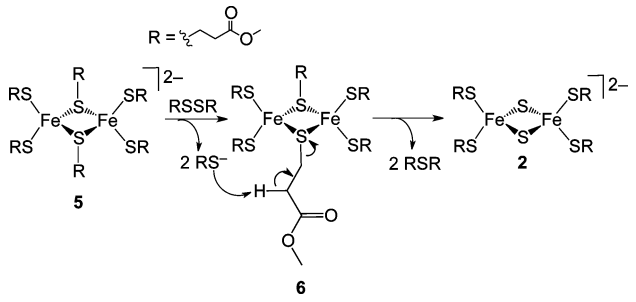

The data obtained thus far have revealed the ability of cysteine analogues to facilitate the conversion of MNICs and $[Fe(SR_4)]^-$ complexes to [2Fe–2S] clusters via a mechanism that relies on the deprotonation of the α-carbon and consequent C–S bond heterolysis. Starting from either MNICs, tetrathiolatoiron(III) complexes, or thiolate-bridged iron(II) dimers, it is possible to form [2Fe–2S] clusters from cysteine analogues, provided that an acidic proton is properly positioned so as to facilitate C–S bond scission.

2.4. Cysteine Analogues Can Convert Tetrathiolatoiron(II) Monomers to [2Fe–2S] Clusters. As described above, our observation of the reactivity of Fe(III) dimers with $(SCH_2CH_2C(O)OMe)_2$ led us to investigate the reactivity of Fe(III) monomers. Tetrathiolatoiron(III) monomers were consequently found to be competent for [2Fe–2S] cluster formation, provided that the thiolate form of the cysteine analogue is present. Given this pattern of reactivity, we reasoned that tetrathiolatoiron(II) monomers may be converted to [2Fe–2S] clusters by $(SCH_2CH_2C(O)OMe)_2$. The oxidation of the Fe(II) center by disulfide generates the equivalent of base (i.e., thiolate) needed to facilitate the C–S cleavage, and no extra base should be needed to generate the [2Fe–2S] cluster.

Indeed, this was found to be the case. UV–vis spectroscopic monitoring experiments demonstrate that addition of $(SCH_2CH_2C(O)OMe)_2$ to a solution of $[Fe(SEt)_4]^{2-}$ (**8b**) leads to the development of the characteristic spectroscopic features of $[Fe_2(\mu\text{-}S)_2(SCH_2CH_2C(O)OMe)_4]^{2-}$ (**2**) (Scheme 8, Supporting Information Figure S10). The reaction could also be carried out on a preparative scale, and the cluster isolated in 85% yield. The use of $[Fe(S^tBu)_4]^{2-}$ (**8a**) instead of the ethyl analogue did not influence the reactivity, and the [2Fe–2S] cluster was isolated in 50% yield. In further analogy to the experiments described above, if **8b** is treated with EtSSEt instead of $(SCH_2CH_2C(O)OCH_3)_2$, the tetrathiolatoiron(III) species is formed, but the reaction does not proceed to cluster. Finally, if **8b** is allowed to react with 1 equiv of ferrocenium, excess MMP, and excess DBN, then the cluster is formed in a 68% yield (Supporting Information Figure S11).

Scheme 8. Mechanism for the Transformation of Tetrathiolatoiron(II) to [2Fe–2S] Cluster

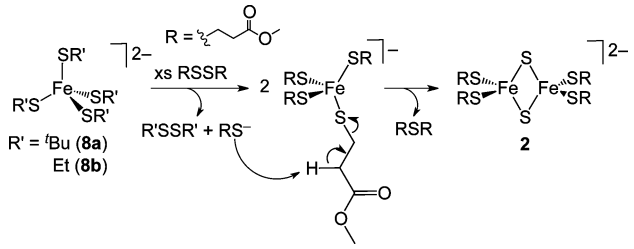

3. SUMMARY AND CONCLUSIONS

[2Fe–2S] clusters can be formed by the reaction of cysteine analogues with mononitrosyl iron complexes (MNICs). An investigation of the mechanism of this reaction has led to the discovery that different Fe(II) and Fe(III) thiolate complexes are also competent to carry out this cysteine-analogue-mediated transformation. The various reactions by which [2Fe–2S] clusters have been observed to form from Fe nitrosyl and iron thiolate species as a result of reaction with a cysteine analogue (or its disulfide) are summarized in Scheme 9.

Scheme 9. Summary of the Reactions by Which [2Fe–2S] Clusters Were Formed in This Paper

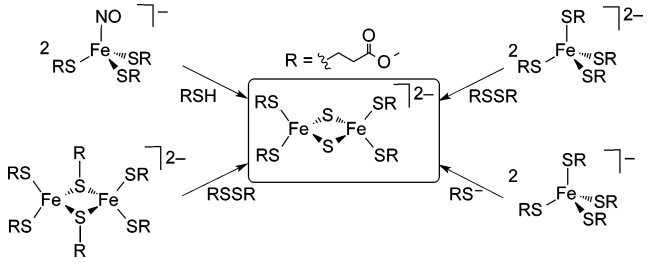

The MNIC-to-[2Fe–2S] cluster transformation relies on the ability of the cysteine analogue to substitute for the initially bound thiolate ligands, release nitric oxide, and undergo base-dependent heterolytic C–S bond cleavage. In addition to MMP, related thiols, such as $HSCH_2CH_2C(O)Me$ and *N*-acetylcysteine methyl ester, were also able to convert MNICs into [2Fe–2S] clusters. Thiolatoiron(II) complexes, either monomeric tetrathiolates or dimers with bridging thiolates, could be converted to [2Fe–2S] clusters using the disulfide forms of these thiolates or sequential addition of an external oxidant and the thiolate. Additionally, monomeric Fe(III) tetrathiolate complexes could be converted to [2Fe–2S] clusters using the thiolate form of cysteine analogues.

These reactions add to the palette of reactivity that is available to chemists exploring iron thiolate complexes and [Fe–S] clusters. More importantly, they also provide valuable insight into the mechanisms of the biochemical transformations that analogous metallocofactors may undergo in biological systems. Importantly, in the long history of investigation into the chemistry of [Fe–S] clusters, the source of the bridging sulfide has typically been elemental S or a sulfide salt such as NaSH. This work shows that a cysteine analogue is sufficient to promote [2Fe–2S] cluster assembly. Moreover, the results presented here provide support for the putative role of MNICs in the transformation of DNICs to [2Fe–2S] clusters. The simplicity of these reactants contrasts sharply with the complexity of the cascade reactions that unfold, but careful

DOI: 10.1021/acs.inorgchem.5b00961
Inorg. Chem. 2015, 54, 10559–10567

analysis of these reactions has provided deeper insight into the inorganic chemistry of these molecules as well as the biochemistry in which they might participate.

4. EXPERIMENTAL SECTION

4.1. General Considerations. Unless otherwise specified, all reactions and manipulations were carried out under an inert atmosphere of nitrogen using an MBraun glovebox (<0.1 ppm of O_2, < 0.1 ppm of H_2O). Fe(II) chloride, Fe(III) chloride, PPNCl, methyl 3-mercaptopropionate (MMP), *N*-acetyl cysteine methyl ester, methyl vinyl ketone, sodium sulfide nonahydrate, 1,5-diazabicyclo[4.3.0]non-5-ene (DBN), diethyl disulfide (EtSSEt), $(SCH_2CH_2OC(O)CH_3)_2$, and ferrocenium hexafluorophosphate ($FcPF_6$) were purchased from Aldrich and used as received. $(SCH_2CH_2C(O)OCH_3)_2$ was purchased from TCI Chemicals and used as received. Solvents were purified by passage over an alumina column under an Ar atmosphere and stored over activated molecular sieves (4 Å). Diethyl ether and tetrahydrofuran were additionally dried over sodium prior to use. Nitric oxide (Matheson, 99%) was purified following a literature method,[49] in which the NO gas stream is passed through an Ascarite column, and then distilled at −80 °C.

4.2. Physical Methods. Unless otherwise specified, samples for spectroscopic analysis were prepared inside a nitrogen glovebox. Infrared spectra were recorded on a Bruker Tensor 27 FTIR Spectrometer. UV−vis spectra were recorded on a Varian Cary 50 Bio spectrometer.

4.3. Synthesis and Reactivity Studies. The compounds $(PPN)_2[Fe(S^tBu)_4]$,[50] $(PPN)_2[Fe(SEt)_4]$,[51] $(PPN)_2[Fe(SPh)_4]$,[52] $(PPN)_2[Fe_2(\mu\text{-}SEt)_2(SEt)_4]$,[44] $(PPN)_2[Fe_2(\mu\text{-}S)_2(S^tBu)_4]$,[53] $(PPN)[Fe(SEt)_4]$,[54] $(PPN)[Fe(S^tBu)_3(NO)]$,[34] $(PPN)[Fe(SEt)_3(NO)]$,[55] $(SCH_2CH_2CH_2C(O)CH_3)_2$,[56] and $HSCH_2CH_2C(O)CH_3$[57] were prepared according to published procedures or with slight modifications.

Synthesis of $(PPN)_2[Fe_2(\mu\text{-}S)_2(SCH_2CH(NHAc)C(O)OMe)_4]$. For method 1, a solution of $(PPN)[Fe(S^tBu)_3(NO)]$ ((PPN)-**1a**) (32 mg, 36 μmol) in 2.0 mL of acetonitrile was transferred to a 10 mL Schlenk flask covered in Al-foil, to which *N*-acetylcysteine-methyl ester (127 mg, 717 μmol) was added at −15 °C. The reaction was allowed to proceed for 2 h over which time the color of the solution changed from red-brown to brown. The volatiles were removed *in vacuo*, and the resulting residue was washed with Et_2O (3 × 1 mL), and 10% v/v MeOH in Et_2O (3 × 1 mL). The residue was then dissolved in 1 mL of cold MeCN. Addition of 15 mL of Et_2O followed by cooling to −38 °C for 12 h induced precipitation of a dark brown powder. This precipitate was filtered and washed with cold Et_2O to afford 13 mg (6.6 μmol, 37%) of $(PPN)_2[Fe_2(\mu\text{-}S)_2(SCH_2CH(NHAc)C(O)OMe)_4]$. For method 2, a solution of $(PPN)_2[Fe_2(\mu\text{-}S)_2(S^tBu)_4]$ (47 mg, 0.029 mmol) in 3.0 mL of THF was transferred to a 10 mL Schlenk flask, to which *N*-acetylcysteine-methyl ester (250 mg, 1.46 mmol) was added at room temperature. The reaction was allowed to proceed for 3 h. The volatiles were removed *in vacuo*, and the residue was washed with Et_2O:MeOH (10:1, 3 × 1 mL). The residue was then dissolved in 1 mL of MeCN. Addition of 15 mL of Et_2O followed by cooling to −38 °C for 12 h induced precipitation of a dark brown powder. This precipitate was filtered and washed with cold Et_2O to afford 33 mg (0.017 mmol, 65%) of $(PPN)_2[Fe_2(\mu\text{-}S)_2(SCH_2CH(NHAc)C(O)OMe)_4]$. UV−vis in MeCN, λ in nm (ε in M^{-1} cm^{-1}): 320 (14 990), 420 (9817), 450 sh (8154). IR (KBr, cm^{-1}): 1745 (s, ν_{CO}), 1669 (s, ν_{CO}), 1513 (s, ν_{CO}), 1115 (w), 724 (w), 693 (w), 533 (w), 499 (s).

Synthesis of $(PPN)_2[Fe_2(\mu\text{-}S)_2(SCH_2CH_2C(O)CH_3)_4]$. For method 1, a solution of $(PPN)[Fe(S^tBu)_3(NO)]$ ((PPN)-**1a**) (8 mg, 9.0 μmol) in 1.0 mL of acetonitrile was transferred to a 10 mL Schlenk flask covered in Al-foil, to which $HSCH_2CH_2C(O)CH_3$ (19 μL, 179 μmol) was injected at −15 °C. The reaction was allowed to proceed for 2 h over which time the color of the solution changed from red-brown to brown. The volatiles were removed *in vacuo*, and the resulting residue was washed with Et_2O (3 × 1 mL), and 10% v/v THF in Et_2O (3 × 1 mL). The residue was then dissolved in 1 mL of cold MeCN. Addition of 15 mL of Et_2O followed by cooling to −38 °C for 12 h induced precipitation of a dark brown powder. This precipitate was filtered and washed with cold Et_2O to afford 3 mg (1.8 μmol, 40%) of $(PPN)_2[Fe_2(\mu\text{-}S)_2(SCH_2CH_2C(O)CH_3)_4]$. For method 2, a solution of $(PPN)_2[Fe_2(\mu\text{-}S)_2(S^tBu)_4]$ (22 mg, 0.014 mmol) in 2.0 mL of MeCN was transferred to a 10 mL Schlenk flask, to which $HSCH_2CH_2C(O)CH_3$ (72 μL, 0.7 mmol) was added at −15 °C. The reaction was allowed to proceed for 2 h. Addition of 15 mL of Et_2O followed by cooling to −38 °C for 12 h induced precipitation of a dark brown powder. This precipitate was filtered and washed with cold Et_2O to afford 5 mg (0.0027 mmol, 20%) of $(PPN)_2[Fe_2(\mu\text{-}S)_2(SCH_2CH_2C(O)CH_3)_4]$. UV−vis in MeCN, λ in nm (ε in M^{-1} cm^{-1}): 320 (25 540), 420 (18 810), 450 sh (16 880). IR (KBr, cm^{-1}): 1702 (s, ν_{CO}), 1264 (s), 1115 (s), 724 (s), 693 (s), 533 (s).

*Reaction of $(PPN)_2[Fe_2(\mu\text{-}SEt)_2(SEt)_4]$ ($(PPN)_2$-**5a**) and $(SCH_2CH_2C(O)OMe)_2$.* An alternative, more laborious procedure for the reaction monitoring and isolation of the reaction products was previously reported.[35] A solution of $(PPN)_2[Fe_2(\mu\text{-}SEt)_2(SEt)_4]$ ($(PPN)_2$-**5a**) (15 mg, 9.6 μmol) in 2.0 mL of THF was transferred to a 10 mL Schlenk flask, to which $(SCH_2CH_2C(O)OCH_3)_2$ (40 μL, 192 μmol) was injected at room temperature. The reaction was allowed to proceed for 5 h over which time a dark-brown powder precipitated. The solid was collected by filtration, washed with THF (5 × 1 mL), and then dissolved in 1 mL of MeCN. Addition of 15 mL of Et_2O followed by cooling to −38 °C for 12 h induced precipitation of a dark brown microcrystalline solid. This precipitate was filtered and washed with cold Et_2O to afford 12 mg (6.8 μmol, 70%) of $(PPN)_2[Fe_2(\mu\text{-}S)_2(SCH_2CH_2C(O)OCH_3)_4]$ ($(PPN)_2$-**2**). Physical characterization (UV−vis and IR spectroscopy) was in agreement with that previously reported for ($(PPN)_2$-**2**).[35]

*Reaction of $(PPN)_2[Fe_2(\mu\text{-}SEt)_2(SEt)_4]$ ($(PPN)_2$-**5a**), $FcPF_6$, MMP, and DBN.* A solution of $(PPN)_2[Fe_2(\mu\text{-}SEt)_2(SEt)_4]$ ($(PPN)_2$-**5a**) (21 mg, 13 μmol) in 2.0 mL of THF was transferred to a 10 mL Schlenk flask, to which $FcPF_6$ (8.9 mg, 26 μmol) was added. After the addition, the solution took on a dark green color. To this solution was injected $HSCH_2CH_2C(O)OMe$ (59 μL, 520 μmol), followed by DBN (33 μL, 260 μmol). The reaction was allowed to proceed for 5 h at room temperature over which time a dark-brown powder precipitated. The solid was collected by filtration, washed with THF (5 × 1 mL), and then dissolved in 1 mL of MeCN. Addition of 15 mL of Et_2O followed by cooling to −38 °C for 12 h induced precipitation of a dark brown microcrystalline solid. This precipitate was filtered and washed with cold Et_2O to afford 11 mg (6.2 μmol, 46%) of $(PPN)_2[Fe_2(\mu\text{-}S)_2(SCH_2CH_2C(O)OCH_3)_4]$ ($(PPN)_2$-**2**). Physical characterization (UV−vis and IR spectroscopy) was in agreement with that previously reported for ($(PPN)_2$-**2**).[35]

*Reaction of $(PPN)_2[Fe_2(\mu\text{-}SEt)_2(SEt)_4]$ ($(PPN)_2$-**5a**), O_2, MMP, and DBN.* A solution of $(PPN)_2[Fe_2(\mu\text{-}SEt)_2(SEt)_4]$ ($(PPN)_2$-**5a**) (20 mg, 13 μmol) in 2.0 mL of THF was transferred to a 10 mL Schlenk flask, to which O_2 (26 μmol) was injected. After 1 min, $HSCH_2CH_2C(O)OCH_3$ (57 μL, 520 μmol), followed by DBN (32 μL, 260 μmol), was injected to the solution. The reaction was allowed to proceed for 12 h at room temperature over which time a dark-brown powder precipitated. The solid was collected by filtration, washed with THF (5 × 1 mL), and then dissolved in 1 mL of MeCN. Addition of 15 mL of Et_2O followed by cooling to −38 °C for 12 h induced precipitation of a dark brown microcrystalline solid. This precipitate was filtered and washed with cold Et_2O to afford 12 mg (6.9 μmol, 53%) of $(PPN)_2[Fe_2(\mu\text{-}S)_2(SCH_2CH_2C(O)OCH_3)_4]$. Physical characterization (UV−vis and IR spectroscopy) was in agreement with that previously reported for $(PPN)_2$-**2**.[35]

*UV−Vis Monitoring of the Reactions of $(PPN)_2[Fe_2(\mu\text{-}SEt)_2(SEt)_4]$ ($(PPN)_2$-**5a**) and RSSR.* In a typical experiment, 0.5−0.9 mM solutions of $(PPN)_2[Fe_2(\mu\text{-}SEt)_2(SEt)_4]$ ($(PPN)_2$-**5a**) in MeCN were prepared in a 2 mm Schlenk cuvette equipped with a rubber septum. The disulfides were injected via syringe and the reactions monitored by their UV−vis spectra at room temperature.

a. $(SCH_2CH_2C(O)OMe)_2$. To a 700 μL solution of $(PPN)_2$-**5a** (0.7 mM) was added $(SCH_2CH_2C(O)OMe)_2$ (5 μL, 25 μmol). The total

DOI: 10.1021/acs.inorgchem.5b00961
Inorg. Chem. 2015, 54, 10559−10567

reaction time was 6 h. The product is consistent with formation of $(PPN)_2[Fe_2(\mu\text{-}S)_2(SCH_2CH_2C(O)OCH_3)_4]$ ($(PPN)_2$-**2**).[35]

b. EtSSEt. To a 700 μL solution of $(PPN)_2$-**5a** (0.9 mM) was added EtSSEt (4 μL, 32 μmol). The total reaction time was 4 h. The product is consistent with formation of $(PPN)[Fe(SEt)_4]$ (**7**).[54]

c. $(SCH_2CH_2CH_2C(O)OMe)_2$. To a 700 μL solution of $(PPN)_2$-**5a** (0.7 mM) was added $(SCH_2CH_2CH_2C(O)OMe)_2$ (6.5 mg, 24.5 μmol). The total reaction time was 5 h. No cluster formation was observed.

d. $(SCH_2CH_2OC(O)Me)_2$. To a 700 μL solution of $(PPN)_2$-**5a** (0.7 mM) was added $(SCH_2CH_2OC(O)Me)_2$ (5 μL, 30 μmol). The total reaction time was 2.5 h. No cluster formation was observed.

*UV−vis monitoring of the reactions of $(PPN)_2[Fe_2(\mu\text{-}SEt)_2(SEt)_4]$ ($(PPN)_2$-**5a**) and Fc^+, MMP, DBN.* To a 700 μL MeCN solution of $(PPN)_2$-**5a** (0.7 mM) was added 108 μL of an MeCN solution of $FcPF_6$ (9.1 mM, 0.98 μmol) at room temperature. The cuvette was gently shaken and the changes in the UV−vis spectra were monitored for 1 min. MMP (2.7 μL, 25 μmol), DBN (3.0 μL, 25 μmol) were then added via syringe and UV−vis spectra were recorded for 20 min. The product is consistent with formation of $(PPN)_2$-**2**.[35]

*Reaction of $(PPN)[Fe(SEt)_4]$ ((PPN)-**7**), $HSCH_2CH_2C(O)OMe$, and DBN.* A solution of $(PPN)[Fe(SEt)_4]$ ((PPN)-7) (21.6 mg, 25.7 μmol) in 1.5 mL of THF was transferred to a 10 mL Schlenk flask, to which MMP (114 μL, 1.03 mmol) and DBN (64 μL, 0.52 mmol) were added. After the addition, the solution immediately took on a red-purple color, and then more slowly turned brown. The reaction was allowed to proceed for 4 h at room temperature over which time a dark-brown powder precipitated. The solid was collected by filtration, washed with THF (5 × 1 mL), and then dissolved in 1 mL of MeCN. Addition of 15 mL of Et_2O followed by cooling to −38 °C for 12 h induced precipitation of a dark brown microcrystalline solid. This precipitate was filtered and washed with cold Et_2O to afford 19.7 mg (11.4 μmol, 89%) of $(PPN)_2[Fe_2(\mu\text{-}S)_2(SCH_2CH_2C(O)OCH_3)_4]$ ($(PPN)_2$-**2**). Physical characterization (UV−vis and IR spectroscopy) was in agreement with that previously reported for $(PPN)_2$-**2**.[35]

*UV−Vis Monitoring of the Reactions of $(PPN)[Fe(SEt)_4]$ ((PPN)-**7**) and RSH.* In a typical experiment, 0.5−0.7 mM solutions of $(PPN)[Fe(SEt)_4]$ ((PPN)-7 in MeCN were prepared in a 2 mm Schlenk cuvette equipped with a rubber septum. The thiols and DBN were injected via syringe and the reactions monitored by their UV−vis spectra at room temperature.

a. $HSCH_2CH_2C(O)OMe$. To a 700 μL solution of (PPN)-7 (0.7 mM) was added $HSCH_2CH_2C(O)OMe$ (2.7 μL, 25 μmol), and DBN (3.0 μL, 25 μmol). The total reaction time was 35 min. The product is consistent with formation of $(PPN)_2$-**2**.[35]

b. $HSCH_2CH_2C(O)Me$. To a 700 μL solution of (PPN)-7 (0.7 mM) was added $HSCH_2CH_2C(O)Me$ (2.5 μL, 25 μmol), and DBN (3.0 μL, 25 μmol). The total reaction time was 4 min, after which time decomposition occurred. The spectral characteristics of the product that formed prior to decomposition are consistent with formation of $(PPN)_2[Fe_2(\mu\text{-}S)_2(SCH_2CH_2C(O)CH_3)_4]$ (Supporting Information Figure S7).

c. N-Acetylcysteine Methyl Ester. To a 700 μL solution of (PPN)-7 (0.5 mM) was added *N*-acetylcysteine methyl ester (3.1 mg, 18 μmol), and DBN (2.2 μL, 18 μmol). The total reaction time was 30 min. The spectral characteristics of the product are consistent with formation of $(PPN)_2[Fe_2(\mu\text{-}S)_2(SCH_2CH(NHAc)C(O)OMe)_4]$ (Supporting Information Figure S9).

Reaction of $(PPN)_2[Fe(SR)_4]$ (R=Et ($(PPN)_2$-8b), ^{t}Bu ($(PPN)_2$-8a)) and $(SCH_2CH_2C(O)OMe)_2$. For R = Et, a solution of $(PPN)_2[Fe(SEt)_4]$ ($(PPN)_2$-**8b**) (22.4 mg, 16.4 μmol) in 2.0 mL of THF was transferred to a 10 mL Schlenk flask, to which $(SCH_2CH_2C(O)OCH_3)_2$ (63 μL, 0.33 mmol) was injected at room temperature. The reaction was allowed to proceed for 5 h over which time a dark-brown powder precipitated. The solid was collected by filtration, washed with THF (5 × 1 mL), and then dissolved in 1 mL of MeCN. Addition of 15 mL of Et_2O followed by cooling to −38 °C for 12 h induced precipitation of a dark brown microcrystalline solid. This precipitate was filtered and washed with cold Et_2O to afford 12 mg (6.7 μmol, 85%) of $(PPN)_2[Fe_2(\mu\text{-}S)_2(SCH_2CH_2C(O)OCH_3)_4]$ ($(PPN)_2$-**2**). Physical characterization (UV−vis and IR spectroscopy) was in agreement with that previously reported for $(PPN)_2$-**2**.[35]

For R = ^{t}Bu, as described for R = Et, a solution of $(PPN)_2[Fe(S^tBu)_4]$ ($(PPN)_2$-**8a**) (28 mg, 18.8 μmol) in 2.0 mL of THF and $(SCH_2CH_2C(O)OCH_3)_2$ (73 μL, 0.66 mmol) yielded 8 mg (4.6 μmol, 50%) of $(PPN)_2$-**2**.

*Reaction of $(PPN)_2[Fe(SEt)_4]$ ($(PPN)_2$-**8b**), $FcPF_6$, MMP, and DBN.* A solution of $(PPN)_2[Fe(SEt)_4]$ ($(PPN)_2$-**8b**) (18.8 mg, 13.6 μmol) in 1.0 mL of THF was transferred to a 10 mL Schlenk flask, to which $FcPF_6$ (4.5 mg, 14 μmol) was added. After the addition, the solution took on a dark red-brown color. To this solution was injected $HSCH_2CH_2C(O)OCH_3$ (75 μL, 0.70 mmol), followed by DBN (84 μL, 0.70 mmol). The reaction was allowed to proceed for 4 h at room temperature over which time a dark-brown powder precipitated. The solid was collected by filtration, washed with THF (5 × 1 mL), and then dissolved in 1 mL of MeCN. Addition of 15 mL of Et_2O followed by cooling to −38 °C for 12 h induced precipitation of a dark brown microcrystalline solid. This precipitate was filtered and washed with cold Et_2O to afford 8.1 mg (4.7 μmol, 68%) of $(PPN)_2[Fe_2(\mu\text{-}S)_2(SCH_2CH_2C(O)OCH_3)_4]$ ($(PPN)_2$-**2**). Physical characterization (UV−vis and IR spectroscopy) was in agreement with that previously reported for $(PPN)_2$-**2**.[35]

*UV−Vis Monitoring of the Reaction of $(PPN)_2[Fe(SEt)_4]$ ($(PPN)_2$-**8b**) and $(SCH_2CH_2C(O)OMe)_2$.* A 700 μL solution of $(PPN)_2[Fe(SEt)_4]$ ($(PPN)_2$-**8b**) (0.6 mM) in MeCN was prepared in a 2 mm Schlenk cuvette equipped with a rubber septum. To this solution was injected a 1.0 M MeCN solution of $(SCH_2CH_2C(O)OMe)_2$ (14 μL, 13 μmol) and the reaction monitored by their UV−vis spectra at room temperature. The total reaction time was 4 h. The product is consistent with formation of $(PPN)_2$-**2**.[35]

*UV−Vis Monitoring of the Reaction of $(PPN)_2[Fe(SEt)_4]$ ($(PPN)_2$-**8b**), $FcPF_6$, MMP, and DBN.* To a 700 μL MeCN solution of $(PPN)_2[Fe(SEt)_4]$ ($(PPN)_2$-**8b**) (0.7 mM) was added 41 μL of an MeCN solution of $FcPF_6$ (12.1 mM, 0.49 μmol) at room temperature. The cuvette was gently shaken, and the changes in the UV−vis spectra were monitored for 1 min. MMP (2.7 μL, 25 μmol) and DBN (3.0 μL, 25 μmol) were then added via syringe, and UV−vis spectra were recorded for 30 min. The product is consistent with formation of $(PPN)_2$-**2**.[35]

■ ASSOCIATED CONTENT

Supporting Information

UV−vis and IR spectra of [2Fe−2S] clusters bearing *N*-acetylcysteine methyl ester and 4-mercaptobutan-2-one. UV−vis titration of $[Fe_2(\mu\text{-}SEt)_2(SEt)_4]^{2-}$ (**5a**) and $FcPF_6$. UV−vis monitoring of a series of reactions including: (i) **5a** and EtSSEt, (ii) $[Fe(SEt)_4]^-$ (**7**) and $HSCH_2CH_2C(O)Me$ with DBN, (iii) **7** and *N*-acetylcysteine methyl ester with DBN, (iv) $[Fe(SEt)_4]^{2-}$ (**8b**) and $(SCH_2CH_2C(O)OMe)_2$, and (v) **8b** and $FcPF_6$ followed by addition of $HSCH_2CH_2C(O)OMe$ with DBN. The Supporting Information is available free of charge on the ACS Publications website at DOI: 10.1021/acs.inorgchem.5b00961.

■ AUTHOR INFORMATION

Corresponding Author

*E-mail: Eunsuk_Kim@brown.edu.

Notes

The authors declare no competing financial interest.

■ ACKNOWLEDGMENTS

The authors thank the Vince Wernig Fellowship (J.F.) and the NSF (E.K., CHE 1254733) for financial support.

DOI: 10.1021/acs.inorgchem.5b00961
Inorg. Chem. 2015, 54, 10559−10567

REFERENCES

(1) Butler, A. R.; Nicholson, R. *Life, Death and Nitric Oxide*; The Royal Society of Chemistry: Cambridge, U.K., 2003.
(2) Ignarro, L. J. *Annu. Rev. Pharmacol. Toxicol.* **1990**, *30*, 535−560.
(3) MacMicking, J.; Xie, Q. W.; Nathan, C. *Annu. Rev. Immunol.* **1997**, *15*, 323−350.
(4) Brenman, J. E.; Bredt, D. S. *Methods. Enzymol.* **1996**, *269*, 119−129.
(5) Ford, P. C.; Lorkovic, I. M. *Chem. Rev.* **2002**, *102*, 993−1018.
(6) Berto, T. C.; Speelman, A. L.; Zheng, S.; Lehnert, N. *Coord. Chem. Rev.* **2013**, *257*, 244−259.
(7) McDonald, C. C.; Phillips, W. D.; Mower, H. F. *J. Am. Chem. Soc.* **1965**, *87*, 3319−3326.
(8) Lewandowska, H.; Kalinowska, M.; Brzoska, K.; Wojciuk, K.; Wojciuk, G.; Kruszewski, M. *Dalton Trans.* **2011**, *40*, 8273−8289.
(9) Tsai, M. L.; Tsou, C. C.; Liaw, W. F. *Acc. Chem. Res.* **2015**, *48*, 1184−1193.
(10) Mallard, J. R.; Kent, M. *Nature* **1964**, *204*, 1192.
(11) Vithayathil, A. J.; Ternberg, J. L.; Commoner, B. *Nature* **1965**, *207*, 1246−1249.
(12) Vanin, A. F.; Nalbandian, R. M. *Biofizika* **1965**, *10*, 167−168.
(13) Cesareo, E.; Parker, L. J.; Pedersen, J. Z.; Nuccetelli, M.; Mazzetti, A. P.; Pastore, A.; Federici, G.; Caccuri, A. M.; Ricci, G.; Adams, J. J.; Parker, M. W.; Lo Bello, M. *J. Biol. Chem.* **2005**, *280*, 42172−42180.
(14) D'Autreaux, B.; Horner, O.; Oddou, J. L.; Jeandey, C.; Gambarelli, S.; Berthomieu, C.; Latour, J. M.; Michaud-Soret, I. *J. Am. Chem. Soc.* **2004**, *126*, 6005−6016.
(15) Kennedy, M. C.; Antholine, W. E.; Beinert, H. *J. Biol. Chem.* **1997**, *272*, 20340−20347.
(16) Lee, M.; Arosio, P.; Cozzi, A.; Chasteen, N. D. *Biochemistry* **1994**, *33*, 3679−3687.
(17) Hyduke, D. R.; Jarboe, L. R.; Tran, L. M.; Chou, K. J.; Liao, J. C. *Proc. Natl. Acad. Sci. U.S.A.* **2007**, *104*, 8484−8489.
(18) Crack, J. C.; Green, J.; Thomson, A. J.; Le Brun, N. E. *Curr. Opin. Chem. Biol.* **2012**, *16*, 35−44.
(19) Ding, H.; Demple, B. *Proc. Natl. Acad. Sci. U.S.A.* **2000**, *97*, 5146−5150.
(20) Tucker, N. P.; Hicks, M. G.; Clarke, T. A.; Crack, J. C.; Chandra, G.; Le Brun, N. E.; Dixon, R.; Hutchings, M. I. *PloS One* **2008**, *3*, e3623.
(21) Yukl, E. T.; Elbaz, M. A.; Nakano, M. M.; Moenne-Loccoz, P. *Biochemistry* **2008**, *47*, 13084−13092.
(22) Kommineni, S.; Yukl, E.; Hayashi, T.; Delepine, J.; Geng, H.; Moenne-Loccoz, P.; Nakano, M. M. *Mol. Microbiol.* **2010**, *78*, 1280−1293.
(23) Smith, L. J.; Stapleton, M. R.; Fullstone, G. J.; Crack, J. C.; Thomson, A. J.; Le Brun, N. E.; Hunt, D. M.; Harvey, E.; Adinolfi, S.; Buxton, R. S.; Green, J. *Biochem. J.* **2010**, *432*, 417−427.
(24) Crack, J. C.; Smith, L. J.; Stapleton, M. R.; Peck, J.; Watmough, N. J.; Buttner, M. J.; Buxton, R. S.; Green, J.; Oganesyan, V. S.; Thomson, A. J.; Le Brun, N. E. *J. Am. Chem. Soc.* **2011**, *133*, 1112−1121.
(25) Drapier, J. C.; Hibbs, J. B., Jr. *J. Clin. Invest.* **1986**, *78*, 790−797.
(26) Drapier, J. C.; Pellat, C.; Henry, Y. *J. Biol. Chem.* **1991**, *266*, 10162−10167.
(27) Yang, W.; Rogers, P. A.; Ding, H. *J. Biol. Chem.* **2002**, *277*, 12868−12873.
(28) Yang, J.; Duan, X.; Landry, A. P.; Ding, H. *Free Radical Biol. Med.* **2010**, *49*, 268−274.
(29) Beinert, H.; Holm, R. H.; Munck, E. *Science* **1997**, *277*, 653−659.
(30) Rao, P. V.; Holm, R. H. *Chem. Rev.* **2004**, *104*, 527−559.
(31) Tran, C. T.; Skodje, K. M.; Kim, E. *Prog. Inorg. Chem.* **2014**, *59*, 339−379.
(32) Tsai, M. L.; Chen, C. C.; Hsu, I. J.; Ke, S. C.; Hsieh, C. H.; Chiang, K. A.; Lee, G. H.; Wang, Y.; Chen, J. M.; Lee, J. F.; Liaw, W. F. *Inorg. Chem.* **2004**, *43*, 5159−5167.
(33) Lu, T. T.; Huang, H. W.; Liaw, W. F. *Inorg. Chem.* **2009**, *48*, 9027−9035.
(34) Harrop, T. C.; Song, D.; Lippard, S. J. *J. Am. Chem. Soc.* **2006**, *128*, 3528−3529.
(35) Fitzpatrick, J.; Kalyvas, H.; Filipovic, M. R.; Ivanovic-Burmazovic, I.; MacDonald, J. C.; Shearer, J.; Kim, E. *J. Am. Chem. Soc.* **2014**, *136*, 7229−7232.
(36) Souza, M. L.; Roveda, A. C., Jr.; Pereira, J. C. M.; Franco, D. W. *Coord. Chem. Rev.* **2015**, DOI: 10.1016/j.ccr.2015.03.008.
(37) Roncaroli, F.; Videla, M.; Slep, L. D.; Olabe, J. A. *Coord. Chem. Rev.* **2007**, *251*, 1903−1930.
(38) Complex **1** was completely consumed upon addition of a single equivalent of MMP to yield unstable nitrosyl species. However, we were not able to characterize it.
(39) Bernasconi, C. F.; Killion, R. B. *J. Am. Chem. Soc.* **1988**, *110*, 7506−7512.
(40) Serjeant, E. P.; Dempsey, B. *Ionization Constants of Organic Acids in Aqueous Solution*; Permagon: Oxford, U.K., 1979.
(41) Warren, J. J.; Tronic, T. A.; Mayer, J. M. *Chem. Rev.* **2010**, *110*, 6961−7001.
(42) Praneeth, V. K. K.; Haupt, E.; Lehnert, N. *J. Inorg. Biochem.* **2005**, *99*, 940−948.
(43) Shearer, J.; Kung, I. Y.; Lovell, S.; Kaminsky, W.; Kovacs, J. A. *J. Am. Chem. Soc.* **2001**, *123*, 463−468.
(44) Hagen, K. S.; Holm, R. H. *J. Am. Chem. Soc.* **1982**, *104*, 5496−5497.
(45) Averill, B. A.; Herskovi, T.; Holm, R. H.; Ibers, J. A. *J. Am. Chem. Soc.* **1973**, *95*, 3523−3534.
(46) Strasdeit, H.; Krebs, B.; Henkel, G. *Inorg. Chem.* **1984**, *23*, 1816−1825.
(47) The estimated[48] pK_a's of the following protons in boldface type are: 24.6 for $HSCH_2C\mathbf{H_2}C(O)OMe$, 36.4 for $HSCH_2C\mathbf{H_2}OC(O)Me$, 25.3 for $HSCH_2CH_2C\mathbf{H_2}C(O)OMe$, 19.6 for $HSCH_2C\mathbf{H_2}C(O)Me$, and 24.6 for $HSCH_2C\mathbf{H}(NHAc)C(O)Me$.
(48) Szegezdi, J.; Csizmadia, F. *Abstr. Pap. Am. Chem. Soc.* **2007**, *233*. The software of the pK_a calculator is commercially available from ChemAxon (Budapest, Hungary).
(49) Schopfer, M. P.; Mondal, B.; Lee, D. H.; Sarjeant, A. A.; Karlin, K. D. *J. Am. Chem. Soc.* **2009**, *131*, 11304−11305.
(50) Ueyama, N.; Sun, W. Y.; Nakamura, A. *Inorg. Chem.* **1992**, *31*, 4053−4059.
(51) Hagen, K. S.; Watson, A. D.; Holm, R. H. *J. Am. Chem. Soc.* **1983**, *105*, 3905−3913.
(52) Hagen, K. S.; Reynolds, J. G.; Holm, R. H. *J. Am. Chem. Soc.* **1981**, *103*, 4054−4063.
(53) Ueno, S.; Ueyama, N.; Nakamura, A.; Tukihara, T. *Inorg. Chem.* **1986**, *25*, 1000−1005.
(54) Maelia, L. E.; Millar, M.; Koch, S. A. *Inorg. Chem.* **1992**, *31*, 4594−4600.
(55) Lu, T. T.; Chiou, S. J.; Chen, C. Y.; Liaw, W. F. *Inorg. Chem.* **2006**, *45*, 8799−8806.
(56) Andrews, C. G.; Langler, R. F.; Branch, D. R. *J. Sulfur Chem.* **2009**, *30*, 22−28.
(57) Ross, N. C.; Levine, R. *J. Org. Chem.* **1964**, *29*, 2346−2350.

DOI: 10.1021/acs.inorgchem.5b00961
Inorg. Chem. 2015, 54, 10559−10567